Organ Polarity in Arabidopsis. NOZZLE Physically Interacts with Members of the YABBY Family[1]

Patrick Sieber[2], Michael Petrascheck[3], Alcide Barberis[4], and Kay Schneitz[5]*

Institute of Plant Biology and Zürich-Basel Plant Science Center, University of Zürich, 8008 Zurich, Switzerland, (P.S., K.S.); and Institute of Molecular Biology, University of Zürich, 8057 Zurich, Switzerland (M.P., A.B.)

Plant lateral organs exhibit proximal-distal and adaxial-abaxial polarity. In Arabidopsis, abaxial cell fate is regulated in part by putative transcription factors of the YABBY family, such as FILAMENTOUS FLOWER (FIL) and INNER NO OUTER (INO), by a mechanism that currently is not fully understood. *NOZZLE (NZZ)* encodes a plant-specific nuclear protein. Genetic evidence has shown that *NZZ* is involved in the positive feedback regulation of *INO*, thereby acting both as a temporal and spatial repressor of *INO* transcription. This mechanism allows the ovule primordium to complete its proximal-distal organization, prior to the onset of adaxial-abaxial development in the chalaza. During our study, we isolated FIL in a yeast two-hybrid screen using NZZ as bait. In vitro pull-down experiments confirmed the NZZ-FIL interaction. NZZ also bound INO and YABBY3, suggesting that NZZ generally interacts with YABBY proteins in vitro. The polar-charged region of NZZ was necessary and sufficient to bind to the zinc finger of INO and to interact with its C terminus carrying the high mobility group-like domain. We suggest that NZZ coordinates proximal-distal patterning and adaxial-abaxial polarity establishment in the developing ovule by directly binding to INO.

Arabidopsis ovules provide an excellent system to study pattern formation in plants (Gasser et al., 1998; Chevalier et al., 2002). Three proximal-distal elements, the funiculus, chalaza, and nucellus, can be distinguished early on (Esau, 1977; Schneitz et al., 1995). After the primordium completes its proximal-distal extension, the inner and outer integuments develop in a sequential fashion. Abaxial outer integument initiation at the chalaza is the first morphological evidence that adaxial-abaxial polarity establishment has occurred and that the radially symmetrically primordium has switched to bilateral development (Baker et al., 1997; Schneitz et al., 1997; Villanueva et al., 1999).

Some progress has recently been made toward the understanding of the molecular mechanism underlying the coordination of proximal-distal and adaxial-abaxial pattern formation in the ovule. In this context, the *INNER NO OUTER* (*INO*) gene, and its regulation, is of central importance. INO belongs to the YABBY family of putative plant-specific transcription factors (Villanueva et al., 1999). Additional members include FILAMENTOUS FLOWER (FIL) and YABBY3 (YAB3; Bowman, 2000). *YABBY* genes are associated with the regulation of abaxial cell fate, by a mechanism which presently is not understood (Bowman and Smyth, 1999; Sawa et al., 1999b; Siegfried et al., 1999; Villanueva et al., 1999). There is evidence coming from in vitro binding studies that FIL protein dimers bind to DNA through their high mobility group (HMG)-like (YABBY) domains in a nonsequence-specific fashion (Kanaya et al., 2002), supporting the idea that YABBY proteins act as transcriptional regulators. Ovules lacking *INO* function only form the inner integument and thus appear radialized (Baker et al., 1997; Schneitz et al., 1997; Villanueva et al., 1999; Balasubramanian and Schneitz, 2000, 2002; Meister et al., 2002). Before the integuments initiate, transcription of *INO* can be detected in a few cells on the abaxial side of the ovule and *INO* expression is subject to a positive autoregulatory loop (Villanueva et al., 1999; Balasubramanian and Schneitz, 2000, 2002; Meister et al., 2002, 2004). Several factors interfering with this process have been identified. *SUPERMAN* (*SUP*), encoding a putative zinc-finger transcription factor (Sakai et al., 1995), is required for abaxial *INO* expression, as in *sup-5* loss-of-function mutants *INO* is misexpressed and *INO* transcription extends into the adaxial chalaza. This causes the loss of unequal outer integument initiation and growth, which eventually leads to a more radialized ovule (Gaiser et al., 1995; Villanueva et al., 1999; Meister et al., 2002). *NOZZLE* (*NZZ*), also known as

[1] This work was supported by the Swiss National Science Foundation (grant nos. 31–53032.97 and 31–65422.01 to K.S.) and by the Kanton of Zürich.

[2] Present address: Division of Biology 156–29, California Institute of Technology, 1200 E. California Blvd., Pasadena, CA 91125.

[3] Present address: HHMI, Fred Hutchinson Cancer Research Center, 1100 Fairview Avenue North, A3–020, P.O. Box 19024, Seattle, WA 98109–1024.

[4] Present address: ESBATech AG, Wagistr. 21, 8952 Zurich-Schlieren, Switzerland.

[5] Present address: Entwicklungsbiologie der Pflanzen, Wissenschaftszentrum Weihenstephan, Technische Universität München, Am Hochanger, 4, 85354 Freising, Germany.

* Corresponding author; e-mail schneitz@wzw.tum.de; fax 49–(0)8161–713337.

Article, publication date, and citation information can be found at www.plantphysiol.org/cgi/doi/10.1104/pp.104.040154.

SPOROCYTELESS, encodes a nuclear protein with limited homology to transcriptional regulators (Schiefthaler et al., 1999; Yang et al., 1999). Previous genetic evidence indicated that *NZZ* coordinates proximal-distal and adaxial-abaxial axis development through the temporal control of *INO* expression and via its involvement in the positive autoregulatory loop of *INO* transcription, which also includes *AINTEGUMENTA* (*ANT*; Balasubramanian and Schneitz, 2000, 2002). *ANT* encodes a transcription factor of the APETALA2 family and is involved in cell proliferation and growth control (Elliott et al., 1996; Klucher et al., 1996; Eshed et al., 1999; Krizek, 1999; Mizukami and Fischer, 2000; Nole-Wilson and Krizek, 2000). In addition to the temporal control of *INO* expression, *NZZ*, together with *ABERRANT TESTA SHAPE* (*ATS*; Léon-Kloosterziel et al., 1994), acts as a spatial repressor of *INO* transcription in the adaxial chalaza, similar to *SUP* (Balasubramanian and Schneitz, 2000, 2002). Thus, *NZZ* acts both as a temporal and spatial repressor of *INO* transcription during ovule development. However, the corresponding molecular mechanism remains to be elucidated. The involvement of *ANT* in the autoregulatory loop of *INO* transcription, as well as the redundancy of *NZZ* and *ATS* in spatially restricting *INO* expression, leave open several possibilities for how the repression of *INO* by *NZZ* can be achieved. In this study, we found the YABBY protein FIL as an interacting partner of NZZ in a yeast two-hybrid screen, and we show that NZZ can interact with several YABBY proteins in vitro, including INO. Our genetic analysis leaves open a possible NZZ-FIL interaction in vivo. By contrast, our observed in vitro NZZ-INO interaction is in accordance with previously reported genetic results. This result indicates that NZZ might coordinate proximal-distal and adaxial-abaxial axis formation in the developing ovule by directly interacting with INO.

RESULTS AND DISCUSSION

NZZ Interacts with FIL in Yeast and In Vitro

We used a yeast two-hybrid approach to identify proteins that interact with NZZ. To overcome potential problems of auto-activation of classical polymerase II reporter genes caused by the bait protein, we used an alternative two-hybrid system, which is based on a polymerase III-transcribed reporter gene (Petrascheck et al., 2001). We screened a cDNA library of approximately 5.8 times 10^6 clones derived from inflorescences containing closed flower buds. Two of the clones that passed the selection contained frag-

Table I. *Plasmid constructs*

Name	Amino Acids	Color Code	Protein	Fused Tag(s)
τ-NZZ	Met-1-Leu-314	N PC MR C	NZZ	τ-138
ΔN$^{1-227}$	Met-1-Tyr-227	N PC MR	ΔNZZ	τ-138
ΔN$^{168-314}$	Ser-168-Leu-314	C	ΔNZZ	τ-138
NZZ	Met-1-Leu-314	N PC MR C	NZZ	GST
ΔN$^{1–148}$	Met-1-Thr-148	N PC MR	ΔNZZ+	GST
ΔN$^{78–148}$	Glu-78-Thr-148	MR	ΔNZZ	GST
ΔN$^{41–148}$	Lys-41-Thr-148	PC MR	ΔNZZ	GST
ΔN$^{1–84}$	Met-1-Ala-84	N PC	ΔNZZ	GST
ΔI$^{1–59}$	Met-1-Val-59	N Zn	ΔINO	Xpress
ΔI$^{1–138}$	Met-1-Ala-138	N Zn MR P	ΔINO	Xpress
ΔI$^{1–174}$	Met-1-Ala-174	N Zn MR P H	ΔINO	Xpress
INO	Met-1-Glu-231	N Zn MR P H C	INO	Xpress
ΔI$^{57–138}$	Leu-57-Ala-138	MR P	ΔINO	Xpress
ΔI$^{138–174}$	Ala-138-Ala-174	H	ΔINO	Xpress
ΔI$^{138–231}$	Ala-138-Glu-231	H C	ΔINO	Xpress
F263	Met-1-Tyr-229	N Zn MR P H C	+FIL	Gal4DBD
F207	Asp-23-Tyr-229	Zn MR P H C	ΔFIL	Gal4DBD
FIL-myc	Met-1-Tyr-229	N Zn MR P H C	FIL	Xpress/MYC
FIL	Met-1-Tyr-229	N Zn MR P H C	FIL	Xpress
YAB3	Met-1-Asn-240	N Zn MR P H C	YABBY3	Xpress

τ-138, τ-138 protein is a cofactor of RNA polymerase III; Gal4pDBD, DNA-binding domain of the Gal4 protein; N, N terminus; PC, polar-charged domain; MR, middle region; C, C terminus; Zn, zinc-finger; P, Pro-rich region; H, HMG-like domain. Δ, Indicates that a truncated form of the protein is used. The YABBY domain contains both the Pro-rich region and the HMG-like domain. The N terminus, the C terminus, and the middle region of NZZ are unrelated to the respective domains of members of the YABBY family. F263 extends further than the first Met of the normal FIL protein by an additional 34 amino acids. F207 is N-terminally truncated by 22 amino acids. Deletion of a single base within the last codon before the stop codon resulted in a frame shift and added 14 amino acids unrelated to NZZ to the C terminus of the ΔN$^{1–148}$ peptide. All tags are fused to the N terminus except for cMYC, which is fused to the C terminus.

ments of the *FIL* cDNA. Both F263 and F207 (see Table I for details of plasmid constructs) contain the full sequence of the YABBY domain (Arg-136-Pro-183; Bowman and Smyth, 1999). Clone F207 starts at residue 23 (Asp-23) with respect to the full-length FIL protein and contains the complete zinc-finger domain according to two reports (Bowman and Smyth, 1999; Villanueva et al., 1999) but does not according to another (Kanaya et al., 2001).

The NZZ protein contains a domain of approximately 40 amino acids in length (Lys-41-Gln-80) toward its N terminus, containing mostly polar or charged residues (Schiefthaler et al., 1999). This polar-charged domain can be subdivided into a basic domain spanning residues 41 to 62 and into a predicted helix domain (residues 63–85; Schiefthaler et al., 1999; Yang et al., 1999). A hydrophobic middle region (Leu-81-Val-146) separates the polar-charged domain

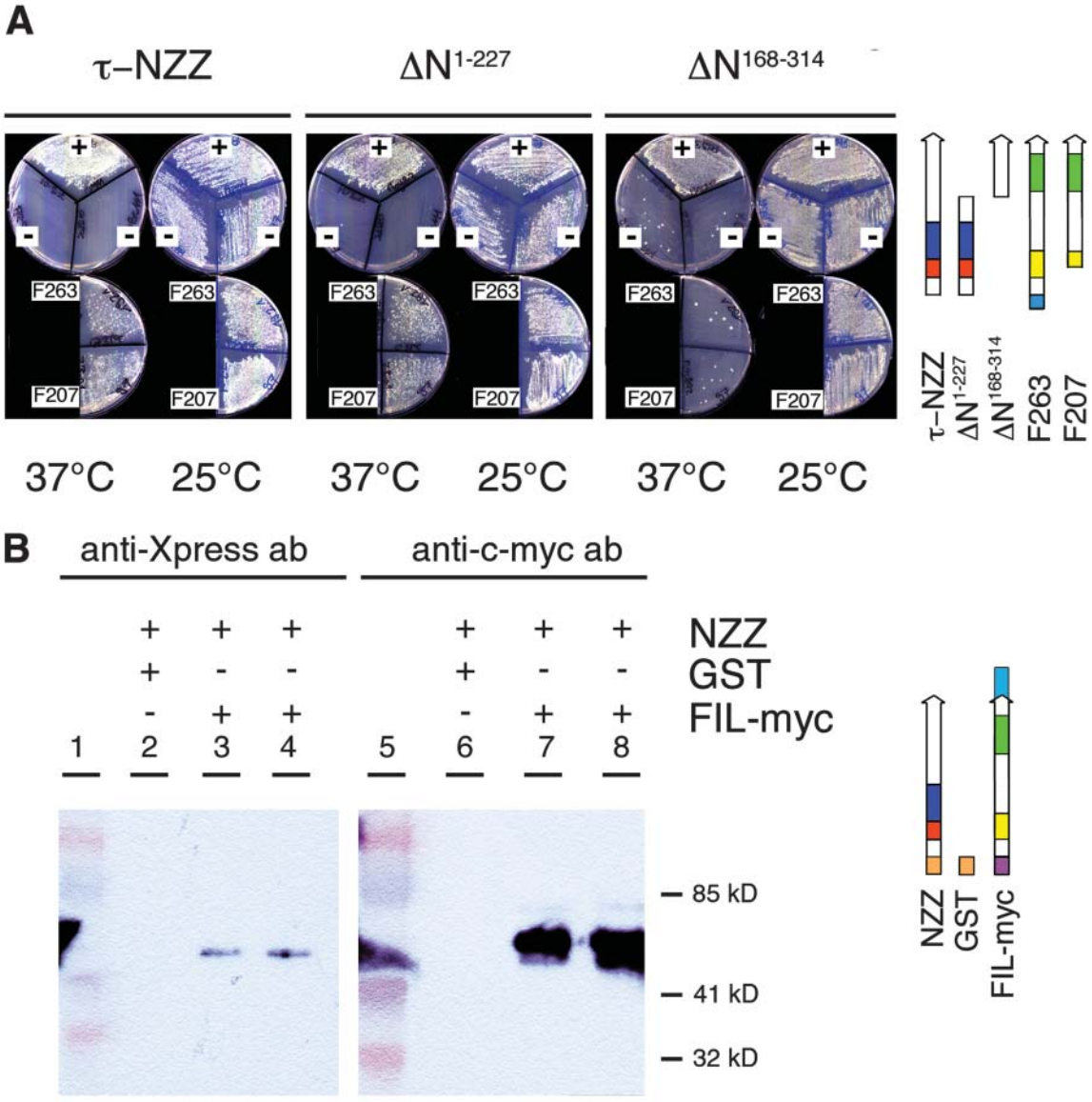

Figure 1. NZZ interacts with FIL in yeast and in vitro. A, Result of yeast two-hybrid screen. The clones FIL207 and FIL263 show interactions that depend on the presence of NZZ protein. Full-length NZZ (τ-NZZ) and the N-terminal fragment of NZZ (ΔN^{1-227}) interact with FIL207 and FIL263, whereas the C terminus of NZZ ($\Delta N^{168-314}$) does not. +, Wild-type *SNR6* was expressed as positive control; −, Gal4pDBD encoding plasmid pPC97 or empty vector yCplac111 were used as negative controls. 25°C and 37°C indicate permissive and restrictive temperature, respectively. B, NZZ and FIL interact in vitro. Two independent pull-down reactions involving GST-NZZ (NZZ) and Xpress/cMYC double-tagged FIL recombinant protein (FIL-myc) were split equally (lanes 3 and 7 and lanes 4 and 8), and the result was detected by using anti-Xpress antibodies (left) and anti-c-myc antibodies (right). FIL-myc is retained by NZZ (lanes 3, 4, 7, and 8) but not by GST (lanes 2 and 6).

from the C terminus. We found that the N terminus of NZZ (ΔN^{1-227}) was necessary and sufficient for the interaction with the fusion proteins F207 and F263 in yeast (Fig. 1A). The C terminus of NZZ ($\Delta N^{168-314}$) was not involved in binding to FIL. The NZZ-FIL protein-protein interaction was confirmed using in vitro pull-down assays (Fig. 1B). NZZ fused to glutathione *S*-transferase (NZZ), but not glutathione *S*-transferase (GST) alone, could bind FIL (Fig. 2, B and C) and Xpress/cMYC double-tagged FIL (FIL-myc), as detected by anti-Xpress and anti-c-myc antibodies, respectively (Fig. 1B).

NZZ Can Interact with Other YABBY Proteins

NZZ was reported to be a spatial and temporal repressor of the *YABBY* gene *INO* (Balasubramanian and Schneitz, 2000, 2002). *INO* expression is restricted to very few cells on the abaxial side of the ovule primordium and to the outer integument (Villanueva et al., 1999; Balasubramanian and Schneitz, 2000, 2002; Meister et al., 2002; Fig. 6B). Thus, *INO* would be difficult to detect in a yeast two-hybrid screen. Therefore, we expressed additional members of the *YABBY* family using in vitro transcription and translation to directly test these proteins for their potential to bind NZZ. *FIL* and *YAB3* represent the most recent gene duplication event within this family, whereas *INO* is more distantly related to *FIL* and *YAB3* (Bowman, 2000). We performed pull-down experiments using GST-NZZ recombinant protein and GST protein alone to detect direct protein-protein interactions with different YABBY proteins. NZZ bound FIL (FIL, FIL-myc), YAB3, and INO reproducibly and independently of GST (Fig. 2, B and C). The interaction of NZZ with INO was proportional to the amount of INO that was added to the reaction (Fig. 2C, lanes 16–18). Thus, NZZ can bind directly to three tested members of the YABBY family, FIL, YAB3, and INO, in vitro, suggesting that NZZ is a general interaction partner of YABBY proteins.

The Polar-Charged Domain of NZZ Is Necessary and Sufficient to Bind INO in Vitro

To map the interaction domain, we performed in vitro pull-down assays combining truncated forms of NZZ with full-length [^{35}S]Met-labeled INO protein (Fig. 3A). We found that INO was retained by all GST-fusion proteins that contained the polar-charged domain of NZZ (Fig. 3A, top, lanes 1, 2, 4, 5, and 6). The middle region of NZZ failed to bind INO (Fig. 3A, top, lane 3), and the N-terminal residues (Met-1-Leu-40) were not necessary for the NZZ-INO interaction (Fig. 3A, top, lanes 4 and 5 versus 6). Neither a Met-to-Val change at residue 64 within the predicted helix of the polar-charged domain nor a Val-to-Ala substitution at residue 29 had an effect on the INO-NZZ protein-protein interaction (Fig. 3A, lanes 4–6).

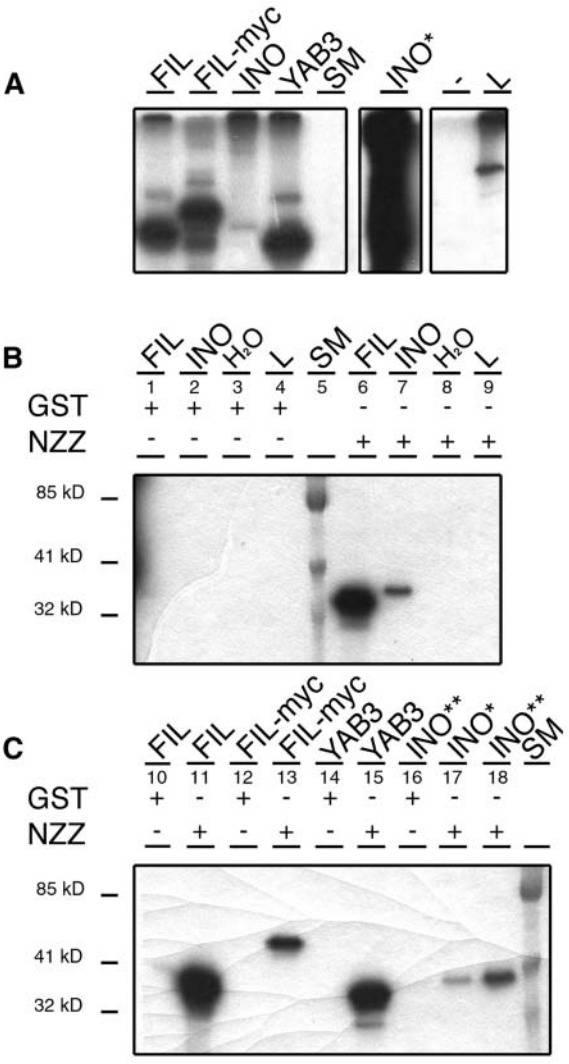

Figure 2. Summary of pull-down reactions. A, *FIL* (FIL, FIL-myc), *INO*, and *YAB3* were transcribed and translated in vitro using [^{35}S]Met in the mix. The SDS-PAGE gel was dried and exposed to an x-ray film. Approximately equal amounts of FIL, FIL-myc, and YAB3 were translated. The amount of translated INO varied in different reactions (compare INO versus INO*). No translation product was detected when empty pRSET plasmid was added (−). The TNT reactions were split, and pull-down assays with equal amounts of GST protein alone or GST-NZZ (NZZ) recombinant protein were performed. B and C, The result of the pull-down reactions is shown on an x-ray film overlaying the dried gel. B, Neither the water control nor the luciferase (L) protein ever produced a signal (lanes 3, 4, 8, and 9). C, NZZ interacts with FIL, FIL-myc, YAB3, and INO, but none of the Xpress-tagged proteins interacts with GST alone (compare lanes 6 and 11 versus 1 and 10; 13 versus 12; 15 versus 14; 7, 17, and 18 versus 2 and 16). INO**, 50 μL of INO* input was used for pull-down reaction (lanes 16 and 18), whereas 20 μL of INO* input was used for pull-down reaction marked INO* (lane 17).

NZZ Can Bind the Zinc-Finger Domain and the C-Terminal Domain of INO in Vitro

INO shares two conserved domains with the other members of the YABBY protein family, a C_2C_2-type zinc finger near the N terminus (Cys-22-Cys-53) and the YABBY domain (Lys-130-His-180; Bowman and Smyth,

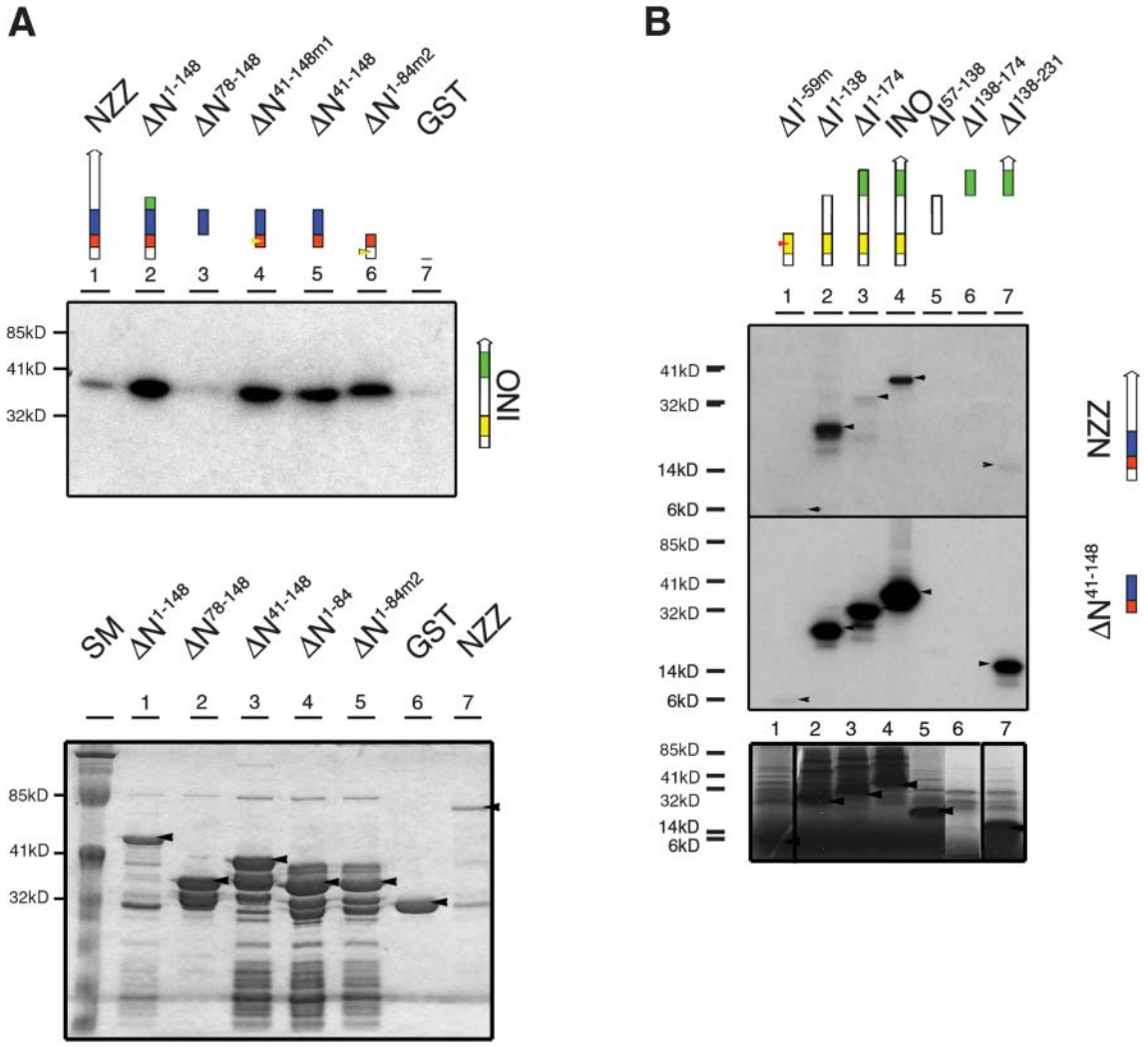

Figure 3. Mapping of the NZZ and INO interaction domains. A, Mapping the INO-binding domain of NZZ. A, top, Result of pull-down reactions. X-ray autoradiograph shows amount of [^{35}S]Met-labeled INO protein, which was retained by various fragments of NZZ protein. A, bottom, Comparable concentrations of ΔN^{1-148}, ΔN^{78-148}, ΔN^{41-148}, ΔN^{1-84}, ΔN^{1-84m2}, and GST (lanes 1–6) as well as $\Delta N^{41-148m1}$ (data not shown) was recovered from glutathione sepharose purified bacterial extracts, as detected on a Coomassie Blue-stained SDS-PAGE. Less GST-NZZ was recovered (lane 7) since NZZ showed a very strong tendency to accumulate in inclusion bodies. Input of the GST-fusion proteins per pull-down reaction was proportional to the input shown in A (bottom). B, Mapping of the NZZ-binding domain(s) of INO. X-ray films are shown in all three sections. B, bottom, Proportional amount of in vitro transcribed/translated fragments of INO protein is shown, as used in pull-down reactions with NZZ (top) and with ΔN^{41-148} (middle). Arrowhead points at band of expected size.

1999; Villanueva et al., 1999), the latter of which is located toward the C-terminal end of the protein. The YABBY domain contains a helix-loop-helix motif with sequence similarity to the first two helices of the HMG domain (Ala-141-Pro-177 or Phe-145-His-180; Bowman and Smyth, 1999; Villanueva et al., 1999). We tested whether NZZ protein can recognize and bind to specific domains of INO. Therefore, we expressed full-length NZZ, as well as a truncated form of NZZ (ΔN^{41-148}), which contained only the polar-charged domain and the middle region fused to GST (Fig. 3A, bottom, lanes 7 and 3, respectively). We used NZZ and ΔN^{41-148} to perform in vitro pull-down assays with several truncated INO proteins. Qualitatively, full-length NZZ and ΔN^{41-148} performed the same with respect to binding INO (compare Fig. 3B, top and middle). Quantitatively, more INO was retained in the pull-down reactions involving the truncated form of NZZ (ΔN^{41-148}; Fig. 3B, top versus middle), likely because more ΔN^{41-148} than NZZ was used per pull-down reaction (see input, Fig. 3A, bottom, lanes 3 versus 7). NZZ and ΔN^{41-148}, both bound to ΔI^{1-138}, ΔI^{1-174}, and INO, all of which share the zinc-finger domain (Fig. 3B, lanes 2–4, respectively). NZZ and ΔN^{41-148}, also bound to ΔI^{1-59m}, but binding was much reduced (Fig. 3B, lane 1 versus 2–4). Subsequent analysis showed that ΔI^{1-59m} contains

a Cys-to-Ser substitution at residue 29 in the zinc-finger domain. Our result indicates that the conserved Cys-29 may be crucial for the folding of the zinc finger (Bowman and Smyth, 1999; Kanaya et al., 2001). We cannot exclude, however, that the lack of the INO middle region in ΔI^{1-59m}, when compared to ΔI^{1-138}, destabilizes the protein and causes the failure to bind NZZ. Still, the middle region (Leu-57-Ala-138), in between the zinc finger and the HMG-like domain, neither bound to NZZ nor to ΔN^{41-148} (Fig. 3B, top and middle, lane 5), indicating that the middle region is not necessary for the NZZ-INO interaction.

The C terminus of INO also interacted with ΔN^{41-148} and with NZZ. The plasmid $\Delta I^{138-231}$ (Ala-138-Glu-231) contained the HMG domain-like helix-loop-helix motif but lacked the Pro-rich region of the YABBY domain. The in vitro transcription and translation of $\Delta I^{138-174}$ failed repeatedly (Fig. 3B, bottom, lane 6). Thus, it is not clear whether the HMG-like domain alone would be sufficient for binding to either NZZ or ΔN^{41-148}. To summarize, NZZ as well as the truncated fragment ΔN^{41-148}, which contained only the polar-charged domain and the middle region, both bound to the conserved zinc finger as well as to the C terminus of INO but not to the less conserved middle region of INO.

Genetic Analysis Leaves Open a Possible In Vivo Interaction of NZZ and FIL

NZZ can interact with FIL, YAB3, and INO in vitro. The NZZ-INO interaction is supported by extensive genetic evidence (Balasubramanian and Schneitz, 2000, 2002). In this section, we present our data that relate to the in vivo relevance of the observed NZZ-FIL interaction. *NZZ* mRNA is present in vegetative tissues, in inflorescences, and in flowers, where *NZZ* transcript accumulates in carpel, stamen, petal, and ovule primordia, as well as in nectaries (Schiefthaler et al., 1999; Fig. 4, A–D, I, and Q). *NZZ* expression in stamens is strongest in the lateral regions of the primordium (Fig. 4, A and B). In stage 2-III ovules, *NZZ* transcript accumulation is strongest in the integuments, but expression can be detected throughout the developing ovule (Schiefthaler et al., 1999; Fig. 4, C, D, and Q). *FIL* is expressed throughout the anlagen of all aboveground lateral organs, but its expression becomes subsequently restricted to the abaxial region of organ primordia (Sawa et al., 1999b; Siegfried et al., 1999). In flowers, *FIL* mRNA accumulates in the abaxial domains of carpels, stamens, petals, and sepals (Sawa et al., 1999b; Siegfried et al., 1999; Fig. 4, E and F). No reproducible expression was detected in ovules (Siegfried et al., 1999; Fig. 4, G and H), even after 5-d exposure of the hybridized slides to the detection reagent (Fig. 4H). Thus, *FIL* and *NZZ* are both expressed in vegetative leaves, and their expression domains in flowers overlap in petal, stamen, and carpel primordia.

The phenotype of loss-of-function *nzz* mutants is mostly restricted to ovule and stamen development (Schiefthaler et al., 1999; Yang et al., 1999; Balasubramanian and Schneitz, 2000; Fig. 5, B, F, and J). Additionally, the inflorescence appears to be more compact (Balasubramanian and Schneitz, 2000). Mutants homozygous for strong *fil* loss-of-function alleles display a range of phenotypes, which mostly concern flower development. Homozygous *fil* mutant flowers are affected in organ number, organ positioning, and organ identity (Chen et al., 1999; Sawa et al., 1999a, 1999b; Siegfried et al., 1999). In the case of *fil* mutants, stamen either arrest as filamentous antherless structures (Fig. 5K1) or occasionally develop one or two locules, which produce fertile pollen (Fig. 5K2). Ovules develop normally in *fil* mutants (Chen et al., 1999; Sawa et al., 1999a; Siegfried et al., 1999; Fig. 5G).Thus, both *NZZ* and *FIL* functions are necessary for normal stamen development. Plants doubly mutant for both *nzz-2* and *fil-5* segregated in the F_2 progeny of a cross between *nzz-2* and *fil-5* in the expected ratio for two recessive Mendelian traits. The *nzz-2 fil-5* doubly homozygous plants were nondistinguishable from *fil-5* single mutants, except for the ovules, which appeared identical to the ovules that developed in the carpels of *nzz-2* mutants (Fig. 5, D, H, L1, and L2). Some stamens of *nzz-2 fil-5* double mutants arrested as radialized filaments (Fig. 5L1). When anthers developed on top of the filament, the anthers appeared flat and were composed of uniformly shaped cells surrounded by epidermal cells (Fig. 5L2; data not shown). Locules never developed and we never observed pollen, as this is also the case for *nzz* single mutants. We did not notice any novel phenotypes in the *nzz-2 fil-5* double mutant plants. The same results were obtained in crosses of *nzz-2* with *fil-1*, *fil-2*, and *fil-3* (data not shown).

FIL is a promoter of abaxial identity; therefore, we examined whether anthers of *nzz-2* mutants show any adaxial-abaxial polarity defects. High-resolution scanning electron micrograph images of the adaxial surface of *nzz-2* anthers show irregularly shaped uniformly sized cells, which typically cover the adaxial anther surface of wild-type stamens (Fig. 4O, upper arrow). The lower arrow points to the gradual change toward files of more elongate cells typical for stamen filaments, indicating some variability in *nzz-2* concerning the anther-filament transition along the proximal-distal axis (see also Fig. 5J). Stomata (Fig. 4P, asterisk) and irregularly shaped cells (Fig. 4P, arrow) are present on the abaxial surface of *nzz-2* anthers, as they are present on the abaxial surface of wild-type anthers (Bowman, 1994). *FIL* expression in *nzz-2* mutant stamen primordia was restricted to the abaxial region and reflected *FIL* expression pattern as seen in wild-type stamens (Fig. 4, M versus E and F). These data indicate that adaxial-abaxial polarity is maintained in *nzz-2* mutant anthers. Regionally restricted accumulation of *FIL* transcript can also be detected in stamens of *fil-5* mutant flowers, indicating that polarity is maintained in some stamens of *fil-5* mutant flowers (Fig. 4N).

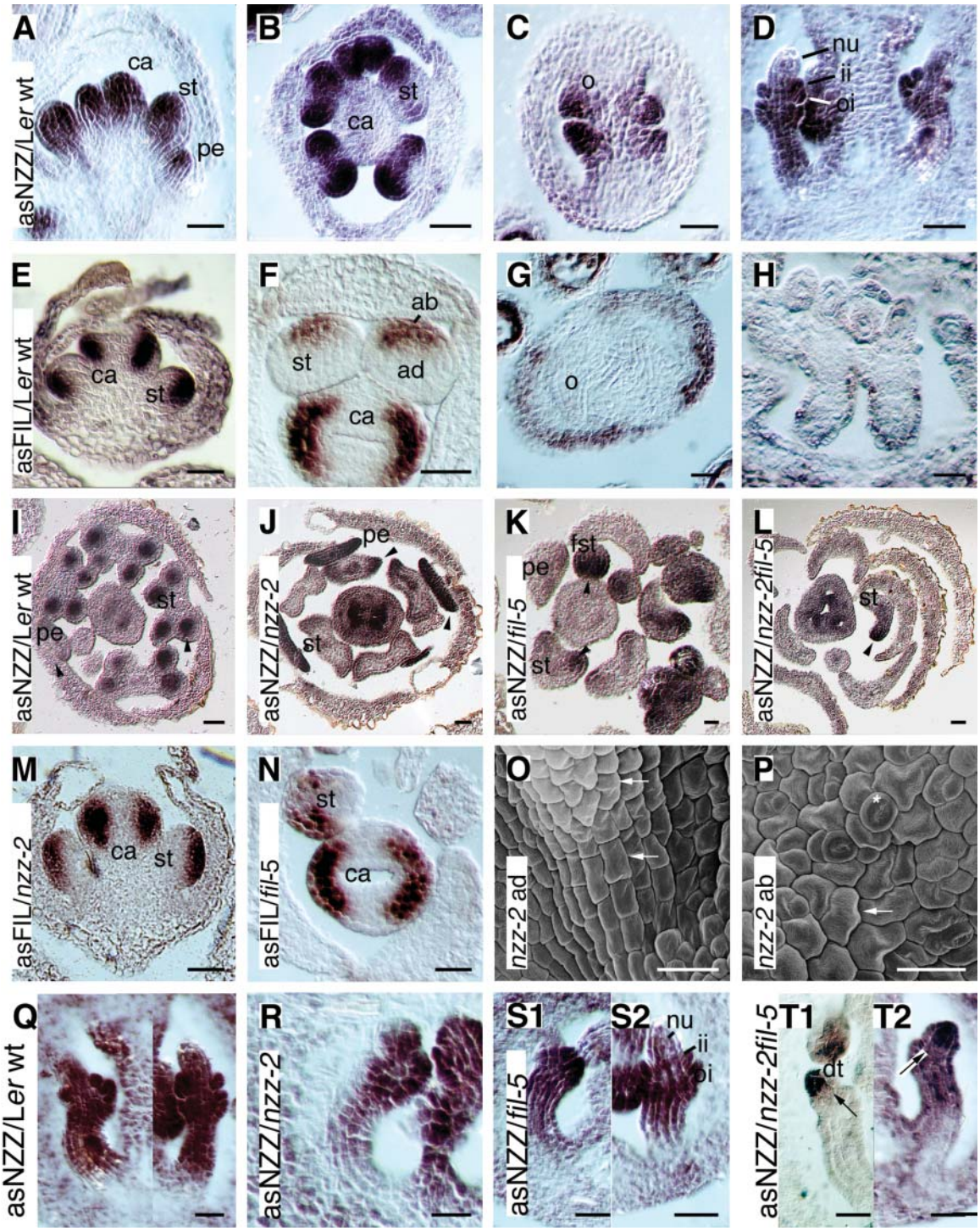

Figure 4. *NZZ* and *FIL* mRNA expression patterns in flowers. RNA in situ hybridization detection of the *NZZ* transcript accumulation in Landsberg *erecta* (A–D, I, Q), *nzz-2* (J, R), *fil-5* (K, S1, S2), and *nzz-2 fil-5* (L, T1, T2) floral tissue. A, Transverse section through stage 7 flower. B, Cross-section through flower around stage 6/7. C, Longitudinal section of stage 1-I ovules developing inside gynoecium. D, Ovules at stage 2-III. E to H, *FIL* mRNA accumulation pattern in wild-type floral organs. E, Longitudinal section through stage 5 flower. F, Transverse section through stage 7 flower. Longitudinal sections of stage 1-II ovules (G) and stage 2-III ovules (H). I to L, Transverse sections through stage 8 flowers of wild-type (I), *nzz-2* (J), *fil-5* (K), and *nzz-2 fil-5* (L) plants. M, Longitudinal section through *nzz-2* mutant flower around stage 5. N, Transverse section through a *fil-5* mutant flower at stage 7. Longitudinal sections through ovules at stage 2-III (Q, S1, S2) and around 2-II/III (R, T1, T2). T1 and T2, Arrows point out elevated levels of *NZZ* transcript accumulation in the distal tip region. O and P, High magnification scanning electron micrograph pictures of the adaxial anther-filament junction (O) and the abaxial surface of anthers (P) of *nzz-2* mutants are shown. O, Upper arrow points to irregularly shaped uniformly-sized cells. The lower arrow points to the gradual change toward files of

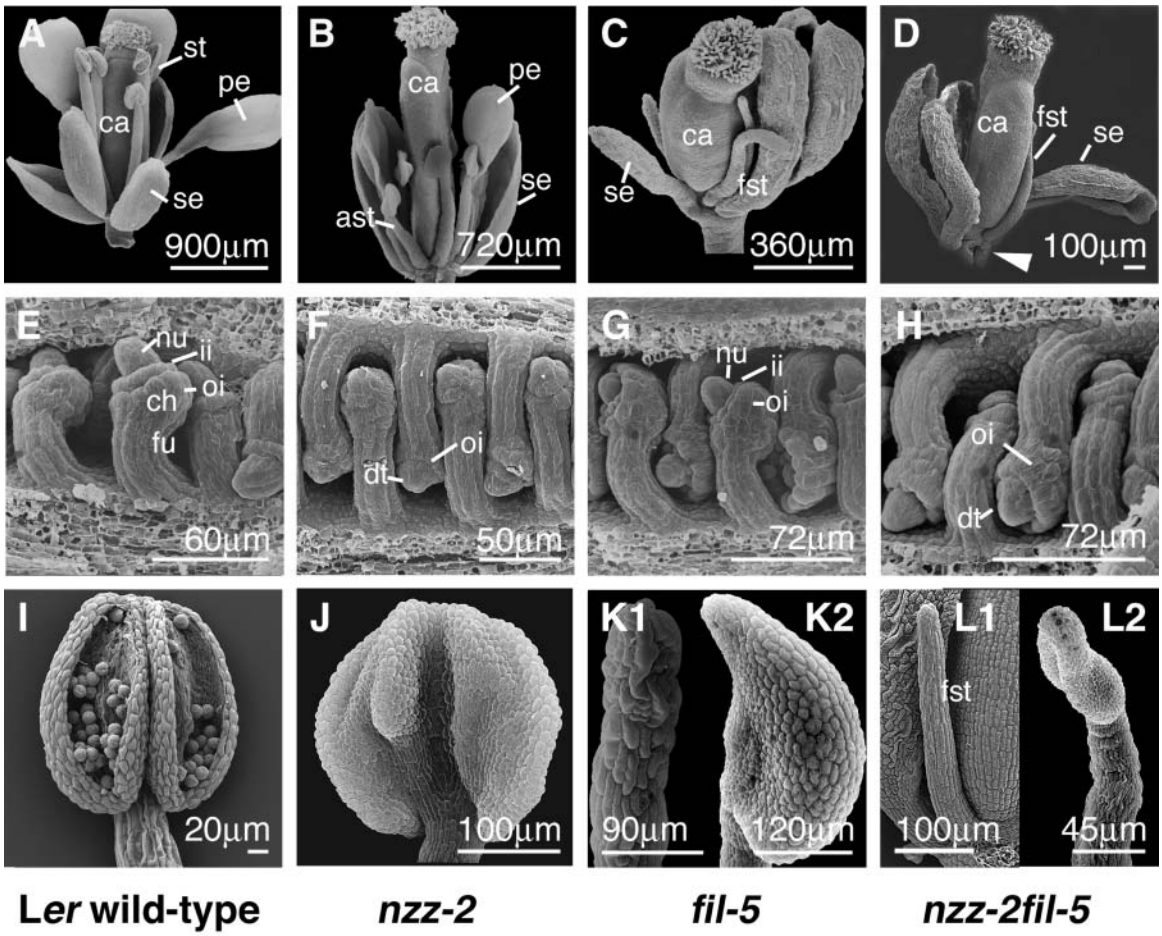

Figure 5. Phenotype of *nzz-2 fil-5* double mutant plants. Scanning electron micrographs of wild-type (A, E, I), *nzz-2* (B, F, J), *fil-5* (C, G, K1, K2), and *nzz-2 fil-5* (D, H, L1, L2) flowers and floral organs. A to D, Flowers around stage 13 are shown. Ovules at stage 2-III (E), 2-IV (G), and around stage 2-II/III (F and H) are shown. I, J, K1, K2, and L2, Anthers of flowers at anthesis (around stage 13) and a filamentous stamen at stage 10 (L1) are shown. Flowers of homozygous *fil-5* (C) plants are affected in organ number, positioning of the floral organs, and in floral organ identity determination (Chen et al., 1999). Flowers of *nzz-2 fil-5* double mutants (D) are almost indistinguishable from *fil-5* (C) single mutants except for the anthers. Anthers of *fil-5* single mutants either arrest as radial filamentous stamens (K1) but occasionally develop one or two fertile locules (K2). Anthers of *nzz-2 fil-5* double mutants never develop locules (compare K2 versus L2) and resemble anthers of *nzz-2* (J). Ovules of *fil-5* mutants develop normally (compare E versus G). Ovules of *nzz-2 fil-5* double mutants (H) resemble *nzz-2* single mutant ovules (F) since they fail to develop a nucellus of normal size. In addition, in both *nzz-2* and *nzz-2 fil-5* ovules, the outer integument initiates prior to the inner integument and initiation of the outer integument occurs distally shifted. ca, carpel; st, stamen; fst, filamentous stamen; ast, arrested stamen; pe, petal; nu, nucellus; dt, distal tip; ch, chalaza; fu, funiculus; ii, inner integument; oi, outer integument; ad, adaxial; ab, abaxial. Arrowhead: A sepal has been removed to give view on the inner organs.

FIL encodes a putative transcriptional regulator, which has been shown to bind DNA in a nonsequence-specific manner (Sawa et al., 1999b; Siegfried et al., 1999; Kanaya et al., 2002). We tested whether *NZZ* expression pattern is dependent on *FIL* function. *NZZ* expression in *fil-5* was detectable in lateral regions of stamen primordia (Fig. 4K), and spatially restricted *NZZ* expression was also detected in filamentous stamens and petals of *fil-5* mutants (Fig. 4K). The distribution of *NZZ* transcript in *nzz-2 fil-5* double mutant flowers resembled the pattern seen in *nzz-2*, *fil-5*, and wild-type flowers (Fig. 4, L versus I–K). Thus, *NZZ* expression in flowers seems to be independent of *FIL* function, except for the ovules, where we found some

Figure 4. (*Continued.*)
more elongate cells typical for filaments. P, Stomata (asterisk) and irregularly shaped cells are present on the abaxial surface of *nzz-2* anthers. ca, carpel; st, stamen; fst, filamentous stamen; pe, petal; o, ovule; nu, nucellus; dt, distal tip; ii, inner integument; oi, outer integument; ad, adaxial; ab, abaxial. Arrowheads points out *NZZ* expression in stamens and petals, respectively. Scale bar = 20 μm. Floral stages after (Smyth et al., 1990) stages of ovule development (Schneitz et al., 1995).

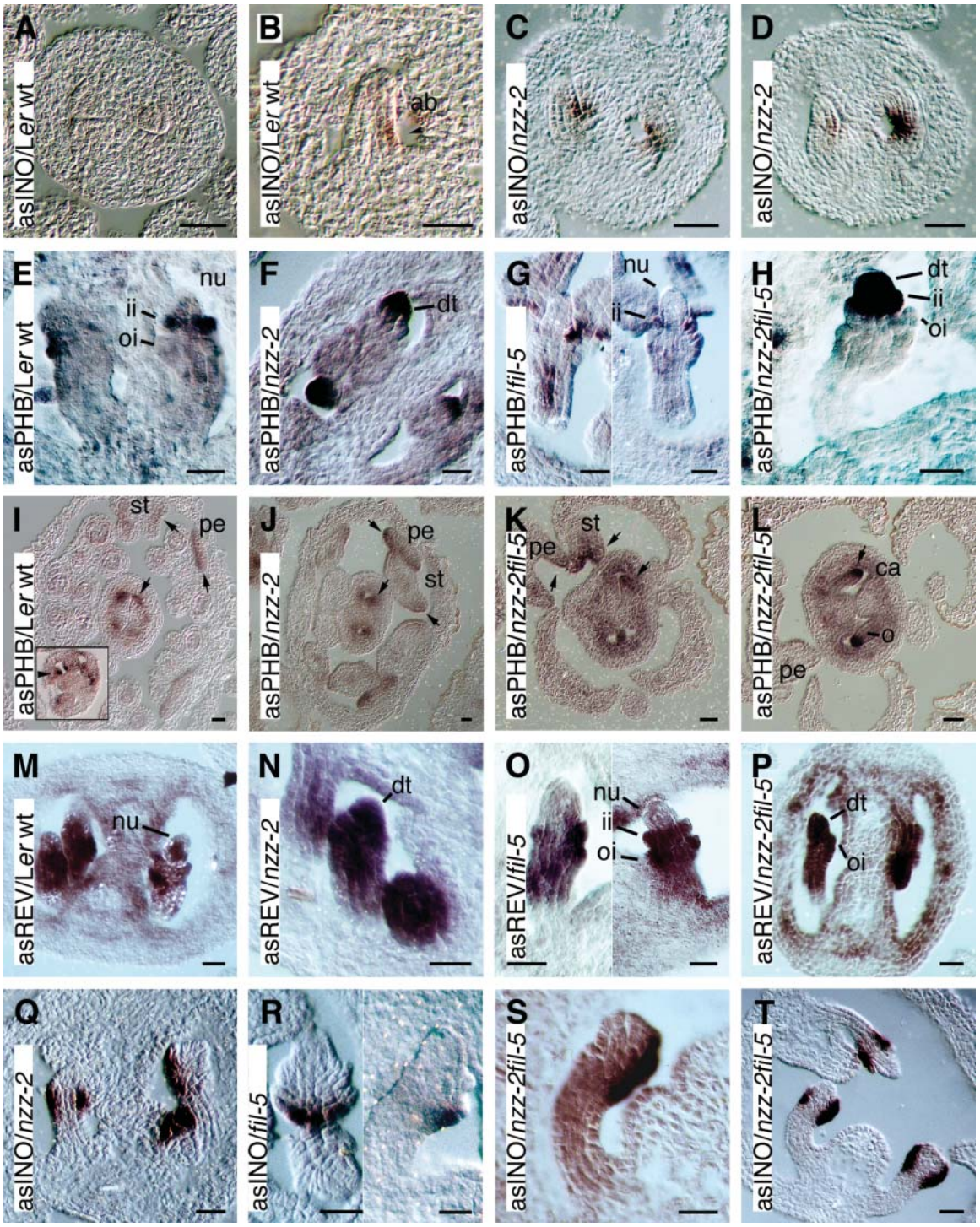

Figure 6. Expression of marker genes in floral organs of wild-type, *nzz-2*, *fil-5*, and *nzz-2 fil-5* double mutant plants. In situ hybridizations of cross-sections through flowers of Landsberg *erecta* (A, B, E, I, M), *nzz-2* (C, D, F, J, N, Q), *fil-5* (G, O, R), and *nzz-2 fil-5* (H, K, L, P, S, T) flowers are shown. *INO* mRNA can be detected in Landsberg *erecta* ovules around stage 2-I (A, B) but slightly earlier (stage 1-II) and at a more distal position in *nzz-2* mutant ovules (C, D; Balasubramanian and Schneitz, 2000, 2002). *INO* expression as detected in transverse sections through ovules at stage 2-III (R) and around stage 2-III (Q, S, T) is shown. *PHB* transcript accumulation, as detected in longitudinal sections through stage 2-III ovules (E–H) and in transverse sections of flowers (I–L). *REV* expression in stage 2-II/2-III ovules is shown (M–P). Arrows point to regions showing high levels of *PHB* transcript accumulation. Scale bar = 20 μm. ab, abaxial; ii, inner integument; oi, outer integument; nu, nucellus; dt, distal tip; st, stamen; pe, petal; ca, carpel; o, ovule.

deviation from the expected *NZZ* expression pattern in *nzz-2 fil-5* double mutants (Fig. 4, T1 and T2). *NZZ* expression was normal in *nzz-2* (Fig. 4, Q versus R; Balasubramanian and Schneitz, 2000) and *fil-5* ovules (Fig. 4, Q versus S1 and S2), respectively. In two independent in situ hybridization experiments, *NZZ* expression appeared up-regulated in the distal tip region of *nzz-2 fil-5* ovules when compared to the level detected in the integuments (Fig. 4, T1 and T2). This result suggests that *FIL* might have a function during ovule development. Thus, both *FIL* and *NZZ* seem to be functionally redundant in preventing the accumulation of high levels of *NZZ* transcript in the nucellus. Although we failed to detect *FIL* mRNA in ovules, *FIL* might be expressed at very low levels in the ovule below the detection limit of in situ hybridization analysis. Alternatively, *FIL* could have some non-cell autonomous effects on ovule development.

FIL function might be masked by the action of its closest homologs in some floral organs, including ovules, but effects of its loss might be detectable as changes seen in the gene expression of some marker genes. Therefore, we examined the expression of *INO*, as well as two additional markers, *PHABULOSA* (*PHB*) and *REVOLUTA* (*REV*), in various floral organs of *nzz-2*, *fil-5*, and *nzz-2 fil-5* double mutants. The latter two are both members of the class III homeodomain Leu-zipper (HD-ZIP) gene family (Zhong and Ye, 1999; Ratcliffe et al., 2000; McConnell et al., 2001; Otsuga et al., 2001). *REV* and *PHB* exhibit similar expression patterns in meristems, in the vasculature, and in adaxial domains of lateral organs (McConnell et al., 2001; Otsuga et al., 2001). *FIL* expression is lost in leaves of homozygous *phb-1d* gain-of-function mutants (Siegfried et al., 1999). Furthermore, it is hypothesized that adaxial and abaxial domains are established in lateral organs by mutual exclusion of the action of class III *HD-ZIP*, as well as the *YABBY/KANADI* gene families from abaxial and adaxial domains, respectively (Eshed et al., 2001; Kerstetter et al., 2001; McConnell et al., 2001; Bowman et al., 2002). A detailed description of the *PHB* expression pattern in ovules and the influence of *NZZ* function on *PHB* transcript accumulation is presented elsewhere (Sieber et al., 2004). Briefly, *PHB* mRNA in the ovule is restricted to the adaxial domain of the emerging ovule primordium (Fig. 6I, arrow) and becomes restricted to the inner integument (Fig. 6E). In ovules of *nzz-2 fil-5* double mutant plants (Fig. 6H), ectopic *PHB* expression can be detected in the distal tip region, as this is the case in *nzz-2* single mutants (Fig. 6F). In *fil-5* mutant ovules (Fig. 6G), as in wild-type ovules (Fig. 6E), *PHB* expression is strongest in the inner integument and *PHB* expression can also be detected in the developing vascular cylinder. During vegetative development, *PHB* mRNA accumulates in the adaxial domain of leaf primordia (McConnell et al., 2001). In flowers, *PHB* expression in petals is stronger in the adaxial domain (Fig. 6I). In stamen primordia most *PHB* transcript is restricted to two lateral regions in the adaxial domain (Fig. 6I, inset, arrowhead). In *nzz-2* mutants (Fig. 6J), *PHB* expression mimics the expression pattern seen in wild-type flowers (I versus J), with an obvious deviation from the normal pattern only detectable in the ovules after stage 1-II/2-I (Fig. 6F). In flowers of *nzz-2 fil-5* double mutant plants (Fig. 6, K and L), elevated *PHB* transcript levels can be detected in distinct regions of petals and stamens, indicating that adaxial identity is maintained to some extent in these organs. Ovules around stage 2-I display the same ectopic *PHB* expression in the distal tip as seen in *nzz-2* single mutant ovules (Fig. 6, L and H versus F). In wild-type ovules, *REV* is expressed throughout the ovule primordium. Strongest *REV* transcript accumu-

Table II. *Primer list*

Primer	Sequence
PS18	CCGGATCCATGGCGACTTCTCTCTTCTTC
PS21	CCGCTAGCTTAAAGCTTCAAGGACAAAT CAATGG
PS35	CCGCTAGCCATAAAGGAAACCTTGGCTCCT
PS42	CCGGATCCTCCAATAATCGCTGTGACACT TGC
PS47	TCCGGATCCCCCAACATGACGACAACACTC
PS48	AATGAATTCTTACTCAAATGGAGATTTTCC
PS67	TCATCGGAAGAGAGTAG
PS85	CGGGATCCAATGTCTATGTCGTCTATGTCC TCC
PS86	GGGGTACCCTTTAATAAGGAGTCACACCA ACG
PS89	CGGGATCCCTTTAATAAGGAGTCACACCA ACG
PS93	CGGAATTCATGTCTATGTCGTCTATGTCC TCC
PS97	CCGAATTCTTAAAGCTTCAAGGACAAATCA ATGG
PS113	CGGGATCCATGTCGAGCATGTCCATG
PS114	CGGAATTCTAGTTATGGGCCACCCCAA
PS121	GGGGTACCAAAGCTATGGAGCAAAAGCTC
PS122	CGGAATTCTTAGGGTACCGAATTCAAGAC CTC
PS123	GGGGTACCATAAGGAGTCACACCAACGTT AGC
PS150	GATCTGGCACGAG
PS151	CTCGTGCCA-5′phosphorylation
PS168	CGGGATCCAAGAGTCGTGGTCGGAAACC
PS169	CGGGATCCGAAAAGAAGCAACTCGCCGCC
PS170	CGGAATTCTTAGGTCTCAACAAAACCCCA TGG
PS171	CGGAATTCTTAGGCGGCGAGTTGCTTCTT TTC
PS172	CGGGATCCATGACAAAGCTCCCCAACATG
PS173	CGGGATCCCTCTCTGTCAATTTGATGAA GGC
PS174	CGGAATTCTTACTCAAATGGAGATTTTCCC
PS175	CGGAATTCTTAGGCCCAATTTTTGGCAGCT AAG
PS176	CGGAATTCTTAAGCTCTTTGTCGCTTCT CAG
PS177	CGGAATTCTTAGACAGAGAGAAGGCTTG TGC
PS178	CGGGATCCGCTCCTTCAGCTTACAATTGC

lation can be seen in both integuments (Fig. 6M). In *nzz-2* (Fig. 6N) and *nzz-2 fil-5* ovules (Fig. 6P), *REV* mRNA accumulates in the distal tip region to levels comparable to the integuments, whereas in *fil-5* ovules, the distribution of *REV* transcript matches the pattern seen in wild type (Fig. 6, O versus M). Thus, except for the expression in the ovules, both *REV* and *PHB* mRNA expression is unaltered in floral organs of *nzz-2* and *nzz-2 fil-5* when compared to wild type. *INO* expression is restricted to the abaxial cell file of the outer integument around stage 2-III. *INO* expression in *fil-5* reflects its wild-type expression pattern, whereas *INO* transcript in ovules of *nzz-2 fil-5* double mutants accumulates in the same pattern as *INO* mRNA in *nzz-2* single mutants (Fig. 6, A–D and Q–T). Thus, *INO*, *PHB*, and *REV* all behave similarly in respect to loss of *NZZ* and *FIL* functions in the flower, respectively.

The expression pattern of the marker genes that we analyzed, namely *INO*, *PHB*, and *REV*, together with the morphological analysis of the *nzz-2 fil-5* double mutant, did not reveal any novel findings in respect to processes that might be regulated by *NZZ* and *FIL* together. However, at this point it is interesting to notice that with *REV* and *PHB*, two members of the class III *HD-ZIP* gene family are prevented from being expressed at high levels in the distal tip region of *nzz-2* mutant ovules. To our knowledge, *NZZ* is thus far the only known factor capable of regulating the spatial distribution of class III *HD-ZIP* transcripts, except for *PHB* itself, and likely the microRNAs miR165/166 (McConnell et al., 2001; Emery et al., 2003; Tang et al., 2003; Juarez et al., 2004; Kidner and Martienssen, 2004).

Taken together, NZZ and FIL may also interact in vivo, as *NZZ* and *FIL* are for example expressed in early stamens and necessary for stamen development (Chen et al., 1999; Sawa et al., 1999a, 1998b; Schiefthaler et al., 1999; Siegfried et al., 1999; Yang et al., 1999). In addition, *FIL* might also have a function in ovule development where it might act redundantly with *NZZ*, thereby acting negatively on *NZZ* transcript levels in the nucellus. However, our genetic analysis of *NZZ* and *FIL* interactions remains inconclusive, and we cannot rule out that the observed NZZ-FIL interaction is not occurring in vivo. Alternatively, a genetic analysis could be complicated by redundancy, as there is extensive genetic redundancy among the *YABBY* genes (Siegfried et al., 1999; Kumaran et al., 2002). In addition, four more homologs of *NZZ* (the homology being restricted to the polar-charged domain) exist in the Arabidopsis genome (P. Sieber, S. Balasubramanian, D. Chevalier, and K. Schneitz, unpublished data).

CONCLUSION

In this study, we show that NZZ can physically interact with three YABBY proteins, FIL, YAB3, and INO, in vitro. Our in vitro binding studies showed that the NZZ protein recognized both the zinc-finger domain as well as the C terminus of INO, including the HMG-like domain. The zinc-finger and the HMG-like domains are conserved among the YABBY proteins, and in the case of FIL the YABBY domain was necessary for in vitro DNA binding (Kanaya et al., 2001, 2002). The polar-charged domain of NZZ was sufficient for binding to INO protein. Thus, the polar-charged domain might recognize YABBY proteins in general.

The Repression of *INO* by *NZZ* Appears To Be Mediated by Direct Protein-Protein Interactions

Extensive genetic evidence indicates that *NZZ* coordinates development of the proximal-distal and adaxial-abaxial axes through the temporal and spatial repression of *INO* allowing proximal-distal axis formation before the initiation of the adaxial-abaxial axis and outer integument development in the chalaza (Balasubramanian and Schneitz, 2000, 2002). First, double mutant analysis showed *ino-2* to be epistatic to *nzz-2*. Second, in *nzz-2* mutant ovules, *INO* expression comes on precociously, correlating with premature formation of the outer integument. Third, *NZZ* and *INO* are coexpressed. Fourth, *NZZ* was shown to be involved in a positive feedback regulatory loop of *INO*. Fifth, *NZZ*, together with *ATS*, is a spatial regulator of *INO* transcription as well. Taken together, the genetic data strongly indicate that *NZZ* and *INO* act in the same pathway and that *NZZ* is a repressor of *INO* (Balasubramanian and Schneitz, 2000, 2002). The data presented in this study corroborate and at the same time extend this model, indicating that the repression of *INO* by *NZZ* involves direct interaction between the two proteins. The new model suggests that NZZ is an inhibitory element of the *INO* autoregulatory loop. Upon initiation of *INO* transcription, NZZ immediately binds freshly translated INO, thus rendering INO inactive. Diminishing functional INO levels attenuate the feedback loop until the repression is overcome by some unknown mechanism. There is evidence that the regulation of *INO* by *SUP* could also take place at the protein level (Meister et al., 2002). At present, it is unclear how the NZZ-INO interaction relates to the role of *NZZ* as a spatial repressor of *INO*, which *NZZ* performs functionally redundant with *ATS* or to the repression mechanism involving *SUP* function (Balasubramanian and Schneitz, 2002; Meister et al., 2002). One future challenge resides in the further elucidation of how these mechanisms relate to each other. Another challenge will be to resolve the basis of the proposed antirepression mechanism involved in the temporal NZZ-INO interaction.

MATERIALS AND METHODS

Plant Materials

Arabidopsis (L.) Heynh. var. Landsberg (*erecta* mutant) was used as wild-type accession. For crosses and in situ hybridization analysis, *nzz-2*, *fil-1*, *fil-2*, *fil-3*, and *fil-5* were used (a kind gift of Garry Drews and John Bowman; Chen et al., 1999; Schiefthaler et al., 1999; Siegfried et al., 1999; Villanueva et al., 1999).

Plasmid Constructs

Standard molecular biological procedures were performed as described (Sambrook and Russell, 2001). An overview of the constructs used is given in Table I.

Yeast Two-Hybrid

The plasmid pHS13#4 (M. Petrascheck and A. Barberis, unpublished data) was digested with *Bam*HI/*Nhe*I, and the insert was eliminated. Full-length *NZZ* cDNA was amplified from the *NZZ* cDNA (Schiefthaler et al., 1999) in a PCR using the primer combination PS18/PS21 (see Table II for details on primer sequences). The digested PCR fragment was then ligated into the *Bam*HI/*Nhe*I-digested pHS13#4 plasmid to generate τ-NZZ. The truncated versions, ΔN^{1-227} as well as $\Delta N^{168-314}$, which represent the N terminus and the C terminus of the NZZ protein, have been produced analogously using primer combinations PS42/PS21 and PS18/PS35, respectively.

GST-Fusion Proteins for In Vitro Pull-Down Assays

The plasmid NZZ was kindly provided by S. Balasubramanian. Truncated versions of NZZ were generated using primer combinations PS18/PS170, PS169/PS170, PS168/PS170, and PS18/PS171. The *Bam*HI/*Eco*RI-digested PCR fragments were cloned in frame to the *GST* coding sequence of the *Bam*HI/*Eco*RI-digested pGEX-4T-2 vector (Amersham Pharmacia, Uppsala) giving rise to ΔN^{1-148}, ΔN^{78-148}, ΔN^{41-148}, and ΔN^{1-84}, respectively. The plasmid pGEX-4T-2 was used to express GST protein, which served as a negative control in the pull-down experiments.

Xpress-Tagged Proteins for In Vitro Pull-Down Assays

The Xpress-tagged proteins FIL, FIL-myc, YAB3, and INO were generated by ligating PCR-amplified and digested cDNAs as translational fusions to the Xpress-tag of pRSET (Invitrogen, Carlsbad, CA). FIL was generated from F263, using primer combination PS85/PS86, and cloned into *Bam*HI/*Kpn*I-digested pRSET. Full-length *YAB3* cDNA was amplified from the Gal4pDBD-cDNA library using PCR primers PS113/PS114. The enzyme combination *Bam*HI/*Eco*RI was used for cloning *YAB3* into pRSET to generate YAB3. *INO* cDNA was amplified from plasmid pRJM23 (kindly provided by Chuck Gasser) using primers PS47/PS48 and cloned into pRSET using *Bam*HI/*Eco*RI to generate INO. Truncated versions of *INO* were constructed analogously with the primer combinations PS172/PS177 to generate ΔI^{1-59}, PS172/PS176 for ΔI^{1-138}, PS172/PS175 for ΔI^{1-174}, PS173/PS176 for ΔI^{57-138}, PS178/ PS175 for $\Delta I^{138-174}$, and PS178/PS174 to produce $\Delta I^{138-231}$, respectively. In order to construct an Xpress-tagged FIL with a cMYC tag fused to its C terminus, we amplified the full-length FIL cDNA from the plasmid F263, using primers PS85/PS123. Six *cMYC* repeats were amplified from the plasmid pGEM::6cMYC (kindly provided by Nicolas Baumberger and Beat Keller) using PCR primers PS121/PS122. We digested the *FIL* cDNA with *Bam*HI/*Asp*718 and ligated the fragment to the *Asp*718/*Eco*RI-digested 6-*cMYC* PCR product. Both fragments were ligated to pRSET, which had been cut with *Bam*HI/*Eco*RI.

In Situ Hybridization

Full-length cDNA of *FIL* was amplified from plasmid F263 using the primer pair PS93/PS89. The PCR fragment was digested with *Bam*HI/*Eco*RI and ligated into the *Bam*HI/*Eco*RI-digested plasmid pSK+ and pKS+ (Stratagene, La Jolla, CA) to generate pSK-FIL and pKS-FIL, respectively. From the clone pSK-FIL, a *Hinc*II fragment of approximately 0.3 kb was excised, and the vector was religated. The resulting pSK-ΔFIL does not contain the YABBY coding sequence (Siegfried et al., 1999). Full-length *NZZ* cDNA was amplified using the primers PS18/PS97 and ligated into *Bam*HI/*Eco*RI-digested pSK+ (Stratagene) to generate pSK-NZZ. *INO* coding sequence was amplified from the plasmid pRJM23 (Villanueva et al., 1999), using the primers PS172 and PS174. After digesting with *Bam*HI and *Eco*RI, full-length *INO* coding sequence was ligated into *Bam*HI/*Eco*RI-digested pSK+ (Stratagene) to generate pSK-INO.

Pol III Yeast Two-Hybrid System

An RNA polymerase III-based yeast two-hybrid system was used for the screen (Petrascheck et al., 2001). The *SNR6* knockout strain MPy15 carries a temperature-sensitive survival construct that allows the strain to grow at 25°C. A second plasmid carries the *UASG-SNR6* reporter gene. Activation of the reporter, caused by the interaction of the fusion protein τ-NZZ with any chimeric Gal4pDBD-Y protein, leads to expression of the wild-type copy of the U6 snRNA. Thus, expression of *SNR6* suppresses the temperature-sensitive phenotype and permits the yeast cells to grow at 37°C (Marsolier and Sentenac, 1999; Petrascheck et al., 2001).

Construction of an Arabidopsis Gal4pDBD-cDNA Library

Polyadenylated mRNA was isolated from Arabidopsis (ecotype Columbia) inflorescences containing flowers up to stage 13 (Smyth et al., 1990), using oligo$(dT)_{25}$-Dynabeads according to the manufacturer's protocol (Dynal, Oslo). Poly(A^+) mRNA, together with marathon cDNA synthesis primer (CLONTECH, Palo Alto, CA) and moloney murine leukemia virus reverse transcriptase, were used for the first-strand synthesis, according to the manufacturer's recommendations (Stratagene). The cDNA termini were blunted after the second-strand synthesis, and a *Bgl*II-adaptor was ligated to the cDNA. For the adaptor, equimolar amounts of the two oligonucleotides PS150 and PS151 were annealed to generate *Bgl*II compatible 5′ overhangs. In a next step, the *Bgl*II ends of the cDNAs were phosphorylated using polynucleotide kinase, and the cDNAs were digested subsequently with *Not*I. This generated cDNAs with *Bgl*II and *Not*I compatible ends, respectively. After size fractionation using SizeSep400 spun columns (Amersham Pharmacia), the cDNAs were ligated into the *Bgl*II- and *Not*I-digested plasmid pPC97 to generate Gal4pDBD-cDNA fusions. The cDNA library in the pPC97 plasmid was then transformed into the XL2-Blue MRF′ ultracompetent *Escherichia coli* strain (Stratagene) and selected on Luria-Bertani medium containing 100 μg mL^{-1} ampicillin. Approximately 9×10^5 colonies were pooled and DNA was isolated, using maxiprep columns, according to the manufacturer's protocol (Genomed, Lohne, Germany).

Yeast Two-Hybrid Screen

The screening strain Mpy15 transformed with plasmid τ-NZZ was cotransformed with the Gal4pDBD-cDNA library. Standard yeast protocols were used with modifications (Petrascheck et al., 2001). Candidate Gal4pDBD-cDNA plasmids were retransformed into the screening strain as well as into MPy15 in order to confirm bait-dependent activation of the reporter gene. The plasmids were sequenced with primer PS67 (see Table II).

Expression of Recombinant Proteins

Recombinant proteins were expressed in BL21 *E. coli* cells (Invitrogen). The bacterial pellet was resuspended in phosphate-buffered saline buffer (137 mM NaCl, 2.7 mM KCl, 10 mM Na_2PO_4, 2 mM KH_2PO_4, pH 7.4) containing protease inhibitor (COMPLETE; Roche Diagnostics, Rotkreuz, Switzerland) and lysed on ice for 30 min with lysozyme (10 μg mL^{-1} final concentration; Roche Diagnostics). The cell lysate was briefly sonicated on ice and centrifuged twice at 4°C with 27,000*g* for 30 min. The supernatant containing the cleared lysate was frozen in aliquots and kept at −80°C until used.

Xpress-tagged (Invitrogen) fusion proteins were expressed using the commercially available TNT quick coupled in vitro transcription/translation system (Promega, Madison, WI) and labeled with [^{35}S]Met (Amersham Pharmacia) according to the manufacturer's recommendations (Promega).

In Vitro Pull-Down Assays

Cleared lysate of BL21 cells expressing GST, NZZ, and truncated versions of NZZ was incubated with Xpress-tagged fusion protein, respectively, and with glutathione sepharose (Amersham Pharmacia) in PBS buffer for 2 h at 4°C on an overhead shaker. After washes, bound proteins were eluted in elution buffer (10 mM reduced glutathione in 50 mM Tris-HCl, pH 8.5) for 30 min on ice.

The eluted samples were mixed 1:1 (v/v) with 2× SDS gel-loading buffer and size separated using SDS-PAGE as described (Sambrook and Russell, 2001). For detecting [^{35}S]Met-labeled proteins, the gel was dried on a Whatman filter paper and exposed to a BIOMAX MR film (Kodak, Rochester, NY) using TRANSCREEN LE intensifying screen (Kodak). Xpress-tagged and cMYC-tagged proteins were detected as described (Spillane et al., 2000; Baumberger

et al., 2001). We used the ECL plus western blotting detection system (Amersham Pharmacia) to monitor peroxidase activity.

In Situ Hybridization Experiments

The in situ hybridization experiments were performed as described (Balasubramanian and Schneitz, 2002). DIG-UTP-labeled sense and antisense *NZZ* RNA probes were in vitro transcribed from *Bam*HI- and *Eco*RI-linearized pSK-NZZ using T7 and T3 polymerase (Roche Diagnostics), respectively. The *FIL* antisense probe lacking the YABBY-domain coding sequence was obtained by transcribing the *Xba*I-digested pSK-ΔFIL with T7 RNA polymerase. Plasmid pKS-FIL was linearized with *Eco*RV and transcribed with T7 RNA polymerase to produce the full-length *FIL* sense probe. Sense and antisense *INO* probes were generated from *Eco*RI- and *Bam*HI-linearized pSK-INO, using T3 and T7 RNA polymerase, respectively. The plasmid pSK-REV#203 was linearized with *Eco*RV and *Sac*I and subsequently transcribed with T3 and T7 RNA polymerase to generate antisense and sense *REV* probe, respectively. The probe contained the identical *REV* fragment as described (Otsuga et al., 2001). Antisense and sense *PHB* probes were made as described (McConnell et al., 2001).

Upon request, all novel materials described in this publication will be made available in a timely manner for noncommercial research purposes, subject to the requisite permission from any third party owners of all or parts of the material. Obtaining any permissions will be the responsibility of the requestor.

ACKNOWLEDGMENTS

We thank John Bowman, Garry Drews, Chuck Gasser, Stephen Clark, Michael Prigge, Kathryn Barton, Sureshkumar Balasubramanian, Nicholas Baumberger, and Beat Keller for sharing mutant seeds and plasmid vectors. Many thanks to Claudia Köhler for technical advice, to members of the Schneitz and the Grossniklaus labs for stimulating discussions, to Jacqueline Gheyselinck and Valeria Gagliardini for technical assistance, and to Frank Wellmer and Elliot Meyerowitz for critical reading of the manuscript.

Received January 31, 2004; returned for revision April 21, 2004; accepted April 25, 2004.

LITERATURE CITED

Baker SC, Robinson-Beers K, Villanueva JM, Gaiser JC, Gasser CS (1997) Interactions among genes regulating ovule development in Arabidopsis thaliana. Genetics **145:** 1109–1124

Balasubramanian S, Schneitz K (2000) *NOZZLE* regulates proximal-distal pattern formation, cell proliferation and early sporogenesis during ovule development in Arabidopsis thaliana. Development **127:** 4227–4238

Balasubramanian S, Schneitz K (2002) *NOZZLE* links proximal-distal and adaxial-abaxial pattern formation during ovule development in Arabidopsis thaliana. Development **129:** 4291–4300

Baumberger N, Ringli C, Keller B (2001) The chimeric leucine-rich repeat/extensin cell wall protein LRX1 is required for root hair morphogenesis in Arabidopsis thaliana. Genes Dev **15:** 1128–1139

Bowman J, editor(1994) *Arabidopsis*: an atlas of morphology and development. Springer Verlag, New York

Bowman JL (2000) The YABBY gene family and abaxial cell fate. Curr Opin Plant Biol **3:** 17–22

Bowman JL, Eshed Y, Baum SF (2002) Establishment of polarity in angiosperm lateral organs. Trends Genet **18:** 134–141

Bowman JL, Smyth DR (1999) *CRABS CLAW*, a gene that regulates carpel and nectary development in Arabidopsis, encodes a novel protein with zinc finger and helix-loop-helix domains. Development **126:** 2387–2396

Chen Q, Atkinson A, Otsuga D, Christensen T, Reynolds L, Drews GN (1999) The *Arabidopsis FILAMENTOUS FLOWER* gene is required for flower formation. Development **126:** 2715–2726

Chevalier D, Sieber P, Schneitz K (2002) The genetic and molecular control of ovule development. *In* S O'Neill, J Roberts, eds, Annual Plant Reviews: Plant Reproduction. Sheffield Academic Press, Sheffield, UK, pp 61–65

Elliott RC, Betzner AS, Huttner E, Oakes MP, Tucker WQ, Gerentes D, Perez P, Smyth DR (1996) *AINTEGUMENTA*, an *APETALA2*-like gene of Arabidopsis with pleiotropic roles in ovule development and floral organ growth. Plant Cell **8:** 155–168

Emery J, Floyd SK, Alvarez J, Eshed Y, Hawker NP, Izhaki A, Baum SF, Bowman JL (2003) Radial patterning of Arabidopsis shoots by class III HD-ZIP and *KANADI* genes. Curr Biol **13:** 1768–1774

Esau K (1977) Anatomy of Seed Plants, Ed 2. John Wiley & Sons, New York

Eshed Y, Baum SF, Bowman JL (1999) Distinct mechanisms promote polarity establishment in carpels of Arabidopsis. Cell **99:** 199–209

Eshed Y, Baum SF, Perea JV, Bowman JL (2001) Establishment of polarity in lateral organs of plants. Curr Biol **11:** 1251–1260

Gaiser JC, Robinson-Beers K, Gasser CS (1995) The *Arabidopsis SUPERMAN* gene mediates asymmetric growth of the outer integument of ovules. Plant Cell **7:** 333–345

Gasser CS, Broadhvest J, Hauser BA (1998) Genetic analysis of ovule development. Annu Rev Plant Physiol Plant Mol Biol **49:** 1–24

Juarez MT, Kui JS, Thomas J, Heller BA, Timmermans MC (2004) microRNA-mediated repression of rolled leaf1 specifies maize leaf polarity. Nature **428:** 84–88

Kanaya E, Nakajima N, Okada K (2002) Non-sequence-specific DNA binding by the FILAMENTOUS FLOWER protein from Arabidopsis thaliana is reduced by EDTA. J Biol Chem **277:** 11957–11964

Kanaya E, Watanabe K, Nakajima N, Okada K, Shimura Y (2001) Zinc release from the CH2C6 zinc finger domain of FILAMENTOUS FLOWER protein from Arabidopsis thaliana induces self-assembly. J Biol Chem **276:** 7383–7390

Kerstetter RA, Bollman K, Taylor RA, Bomblies K, Poethig RS (2001) KANADI regulates organ polarity in Arabidopsis. Nature **411:** 706–709

Kidner CA, Martienssen RA (2004) Spatially restricted microRNA directs leaf polarity through ARGONAUTE1. Nature **428:** 81–84

Klucher KM, Chow H, Reiser L, Fischer RL (1996) The *AINTEGUMENTA* gene of Arabidopsis required for ovule and female gametophyte development is related to the floral homeotic gene *APETALA2*. Plant Cell **8:** 137–153

Krizek BA (1999) Ectopic expression of *AINTEGUMENTA* gene results in increased growth of floral organs. Dev Genet **25:** 224–236

Kumaran MK, Bowman JL, Sundaresan V (2002) *YABBY* polarity genes mediate the repression of *KNOX* homeobox genes in Arabidopsis. Plant Cell **14:** 2761–2770

Léon-Kloosterziel KM, Keijzer CJ, Koornneef M (1994) A seed shape mutant of *Arabidopsis* that is affected in integument development. Plant Cell **6:** 385–392

Marsolier MC, Sentenac A (1999) RNA polymerase III-based two-hybrid system. Methods Enzymol **303:** 411–422

McConnell JR, Emery J, Eshed Y, Bao N, Bowman J, Barton MK (2001) Role of *PHABULOSA* and *PHAVOLUTA* in determining radial patterning in shoots. Nature **411:** 709–713

Meister RJ, Kotow LM, Gasser CS (2002) *SUPERMAN* attenuates positive *INNER NO OUTER* autoregulation to maintain polar development of Arabidopsis ovule outer integuments. Development **129:** 4281–4289

Meister RJ, Williams LA, Monfared MM, Gallagher TL, Kraft EA, Nelson CG, Gasser CS (2004) Definition and interactions of a positive regulatory element of the Arabidopsis *INNER NO OUTER* promoter. Plant J **37:** 426–438

Mizukami Y, Fischer RL (2000) Plant organ size control: *AINTEGUMENTA* regulates growth and cell numbers during organogenesis. Proc Natl Acad Sci USA **97:** 942–947

Nole-Wilson S, Krizek BA (2000) DNA binding properties of the *Arabidopsis* floral development protein *AINTEGUMENTA*. Nucleic Acids Res **28:** 4076–4082

Otsuga D, DeGuzman B, Prigge MJ, Drews GN, Clark SE (2001) *REVOLUTA* regulates meristem initiation at lateral positions. Plant J **25:** 223–236

Petrascheck M, Castagna F, Barberis A (2001) Two-hybrid selection assay to identify proteins interacting with polymerase II transcription factors and regulators. Biotechniques **30:** 296–298, 300, 302

Ratcliffe OJ, Riechmann JL, Zhang JZ (2000) *INTERFASCICULAR FIBERLESS1* is the same gene as *REVOLUTA*. Plant Cell **12:** 315–317

Sakai H, Medrano LJ, Meyerowitz EM (1995) Role of *SUPERMAN* in maintaining Arabidopsis floral whorl boundaries. Nature **378:** 199–203

Sambrook J, Russell DW (2001) Molecular Cloning: A Laboratory Manual, Ed 3. Cold Spring Harbor Laboratory Press, Cold Spring Harbor, NY

Sawa S, Ito T, Shimura Y, Okada K (1999a) *FILAMENTOUS FLOWER*

controls the formation and development of Arabidopsis inflorescences and floral meristems. Plant Cell **11:** 69–86

Sawa S, Watanabe K, Goto K, Kanaya E, Morita EH, Okada K (1999b) *FILAMENTOUS FLOWER* a meristem and organ identity gene of *Arabidopsis* encodes a protein with a zinc finger and HMG-related domains. Genes Dev **13:** 1079–1088

Schiefthaler U, Balasubramanian S, Sieber P, Chevalier D, Wisman E, Schneitz K (1999) Molecular analysis of *NOZZLE*, a gene involved in pattern formation and early sporogenesis during sex organ development in Arabidopsis thaliana. Proc Natl Acad Sci USA **96:** 11664–11669

Schneitz K, Hulskamp M, Kopczak SD, Pruitt RE (1997) Dissection of sexual organ ontogenesis: a genetic analysis of ovule development in Arabidopsis thaliana. Development **124:** 1367–1376

Schneitz K, Hülskamp M, Pruitt RE (1995) Wild-type ovule development in Arabidopsis thaliana: a light microscopy study of cleared whole-mount tissue. Plant J **7:** 731–749

Sieber P, Gheyselinck J, Gross-Hardt R, Laux T, Grossniklaus U, Schneitz K (2004) Pattern formation during early ovule development in *Arabidopsis thaliana*. Dev Biol (in press)

Siegfried KR, Eshed Y, Baum SF, Otsuga D, Drews GN, Bowman JL (1999) Members of the *YABBY* gene family specify abaxial cell fate in Arabidopsis. Development **126:** 4117–4128

Smyth DR, Bowman JL, Meyerowitz EM (1990) Early flower development in Arabidopsis thaliana. Plant Cell **2:** 755–767

Spillane C, MacDougall C, Stock C, Kohler C, Vielle-Calzada JP, Nunes SM, Grossniklaus U, Goodrich J (2000) Interaction of the Arabidopsis polycomb group proteins FIE and MEA mediates their common phenotypes. Curr Biol **10:** 1535–1538

Tang G, Reinhart BJ, Bartel DP, Zamore PD (2003) A biochemical framework for RNA silencing in plants. Genes Dev **17:** 49–63

Villanueva JM, Broadhvest J, Hauser BA, Meister RJ, Schneitz K, Gasser CS (1999) *INNER NO OUTER* regulates abaxial-adaxial patterning in Arabidopsis ovules. Genes Dev **13:** 3160–3169

Yang WC, Ye D, Xu J, Sundaresan V (1999) The *SPOROCYTELESS* gene of Arabidopsis is required for initiation of sporogenesis and encodes a novel nuclear protein. Genes Dev **13:** 2108–2117

Zhong R, Ye Z-H (1999) *IFL1*, a gene regulating interfascicular fiber differentiation in Arabidopsis encodes a homeodomain-leucine zipper protein. Plant Cell **11:** 2139–2152